

Development of a Semiconductor-Based Electrochemical Sensor for Interferon- γ Detection

Zhihui Chu, Haiyan Dai, Yingwei Liu and Yuhua Lin*

Department of Ophthalmology, Hongqi Hospital Affiliated to Mudanjiang Medical University, No.5 Tongxiang Rd, Aimin, Mudanjiang, Heilongjiang, 157000, P.R. China

*E-mail: linyuhua36@163.com

Received: 12 July 2017 / *Accepted:* 26 August 2017 / *Published:* 12 September 2017

This report described an excellent method for interferon gamma (IFN γ) detection using a label-free electrochemical impedance immunosensor. TiO₂ NPs prepared using a simple hydrothermal strategy were applied to the immobilization of the IFN γ monoclonal antibody. The relative increase in the impedance value was proportional to the logarithmic value of the IFN γ concentration (0.001 - 0.2 ng/mL), and the limit of detection (LOD) was calculated as 0.74 pg/mL. This work presented a facile, novel and highly sensitive strategy.

Keywords: Interferon gamma; Semiconductor; TiO₂ NPs; Immunosensor; Electrochemical impedance spectroscopy

1. INTRODUCTION

Lymphocytes from the orbital tissues of patients affected by Graves' ophthalmopathy (GO) or from thyroid tissues of patients with Graves' disease (GD) exhibit a dominant helper T cell type 1 (Th1) profile, while a vast majority of the lymphocytes from patients with remote-onset GO [1, 2] show a Th2 profile [3]. These clinical observations, along with the observed production of substantial CXCL10 by human thyrocytes in primary cultures under interferon- γ (IFN γ)-induced stimulation, indicate that the autoimmune response can be modulated by thyroid follicular cells via the production of CXCL9/Mig and CXCL10 [4-7]. The migration of Th1 lymphocytes to the gland could be facilitated by these chemokines, where IFN γ is secreted. Conversely, the production of chemokine by follicular cells could be stimulated by IFN γ , leading to the perpetuation of the autoimmune process [8]. Other autoimmune disorders might be explained by the above pathogenetic hypothesis. Particularly, the pathogenesis of GO might involve a similar mechanism if orbital fibroblasts and orbital

preadipocytes from GO-p secreted CXCL10 under IFN γ /TNF α stimulation. Hence IFN γ detection is of vital significance for the diagnostics of GO.

A label-free strategy based on electrochemical impedance spectroscopy (EIS) is proposed for the direct determination of immunospecies through the measurement of the impedance variation, since a majority of antigen and antibody molecules are electrochemically inert [9-11]. This strategy could decrease the cost of measurement by eliminating the need for extra materials (i.e., labelled antibodies) during determination. Furthermore, the EIS measurement functions as a non-destructive technique for characterizing the electrical characteristics of a biological interface [12-14]. Electrochemical impedance immunosensors have recently gained extensive attention in numerous biological reports [15-23].

In this report, a new electrochemical impedance immunosensor based on the immobilization of the IFN γ monoclonal antibody on a TiO $_2$ -modified electrode was initially proposed for highly sensitive IFN γ detection. The sensitivity of our developed immunosensor was enhanced by the loading of proteins, which was achieved on the desirable, hydrophilic, and high capacity platform provided by TiO $_2$. The relative increase of the impedance value corresponding to the specific reaction between the IFN γ antibody and IFN γ was measured for the determination of IFN γ . The proposed strategy was confirmed to be highly sensitive, simple, and lower cost compared with the traditional measurement methods.

2. EXPERIMENTS

2.1. Chemicals

Absolute ethanol, hydrazine, and titanium(IV) bis(ammonium lactato)dihydroxide were commercially available from Sinopharm Chemical Reagent Co., Ltd. Purified monoclonal IFN- γ antibody and purified recombinant IFN- γ antigen were commercially available from the Shandong Agricultural Research Institute. Bovine serum albumin (BSA) and Nafion were commercially available from Sigma. The proportion of Na $_2$ HPO $_4$ and NaH $_2$ PO $_4$ was adjusted to obtain a 0.1 M pH 7.0 phosphate buffered saline (PBS buffer). All other chemicals were of analytical reagent grade and were prepared with distilled water.

2.2. Preparation of TiO $_2$ nanoparticles

The synthesis of the TiO $_2$ nanoparticles used in this study was performed based on the simple hydrothermal technique proposed by Lui and co-workers [24] with several alterations. Acetic acid (20 mL) was mixed with titanium butoxide (2 mL) and stirred for 30 min. This step was followed by introducing the mixture into a Teflon-lined stainless-steel autoclave (50 mL), heating the mixture to 150 °C for 10 h, and finally, natural cooling the mixture to ambient temperature. Then, the product was centrifuged to collect the sediment, which was then washed. After heating to 500°C, TiO $_2$ nanoparticles were obtained.

2.3. Preparation of IFN γ immunosensor

After successive polishing using an alumina slurry (0.03 and 0.05 μm), a glassy carbon electrode (GCE) was completely rinsed with distilled water, followed by sonication in nitric acid–water (1:1 v/v), ethanol and distilled water, and then air drying. Afterwards, the as-prepared TiO₂ NPs (2.0 mg) were dispersed in distilled water (1.0 mL) and ultrasonically stirred, followed by the addition of monoclonal IFN γ antibody (0.5 mL, 400 $\mu\text{g}/\text{mL}$) to the TiO₂ NPs suspension (0.5 mL) (denoted anti-IFN γ /TiO₂/GCE). Then, 5.0 μL of the final mixed solution was dropped onto the pre-treated GCE and allowed to stand for 12 h at 4 °C. This was followed by dropping Nafion (5.0 μL , 1.0%) onto the antibody-embedded GCE surface to prevent leakage of the IFN γ antibody from the TiO₂ NP/GCE. Subsequently, a BSA solution (10 mg/mL) was introduced at 37.5 °C for 0.5 h to block the non-specific sites (denoted as BSA/anti-IFN γ /TiO₂/GCE). The IFN γ immunosensor was obtained after washing with PBS three times and stored at 4 °C for further application (denoted IFN γ /BSA/anti-IFN γ /GCE).

2.4. Immunoassay measurement

A CHI 660D electrochemical workstation (CH Instruments, Shanghai, China) was used for all electrochemical measurements with a traditional triple-electrode configuration. The working, reference, and auxiliary electrodes consisted of the original or decorated GCE (diameter, 3 mm), a saturated calomel electrode (SCE), and a platinum wire, respectively. EIS and CV measurements were performed in PBS containing K₃[Fe(CN)₆]/K₄[Fe(CN)₆] (5.0 mM) and KCl (0.1 M), and the scan rate was 100 mV/s. EIS measurements were conducted over a frequency range of 10⁻¹ - 10⁵ Hz at an amplitude of 10 mV for the applied sine wave potential.

3. RESULTS AND DISCUSSION

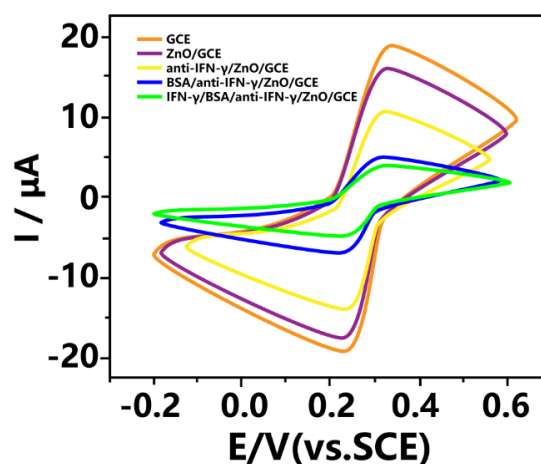


Figure 1. Cyclic voltammograms (CVs) of the original GCE, the TiO₂-modified GCE, the anti-IFN γ /TiO₂-modified GCE, the BSA/anti-IFN γ /TiO₂-modified GCE and the IFN γ /BSA/anti-IFN γ -modified TiO₂/GCE in a 0.1 M pH 7.0 PBS solution containing KCl (0.1 M) and K₃[Fe(CN)₆]/K₄[Fe(CN)₆] (5.0 mM) at a scan rate of 50 mV/s.

The performance of the electrode after each fabrication step was studied using CV measurements. The $\text{Fe}(\text{CN})_6^{3-/4-}$ redox reaction at the original GCE, the TiO_2 -modified GCE, the anti-IFN γ / TiO_2 -modified GCE, the BSA/anti-IFN γ / TiO_2 -modified GCE and the IFN γ /BSA/anti-IFN γ / TiO_2 -modified GCE was characterized via the CVs shown in Fig. 1. Compared to the original GCE, a gradual decrease in the redox current was observed after the stepwise modifications, indicating an impeded electron transfer process between the surface of the GCE and the $\text{Fe}(\text{CN})_6^{3-/4-}$ probe. Particularly, the charge transfer was blocked to a greater degree at the GCE after the immobilization of BSA and the IFN γ antibody, suggesting that the current of the cathodic and anodic peaks was sharply decreased. The introduction of BSA improved the interaction between the IFN γ antibody and TiO_2 because sufficient space for IFN- γ binding was secured by competitive immobilization [25].

In Fig. 2, the strategy for IFN γ determination is presented in detail. After incubation with the IFN γ antigen (varying concentrations) for 80 min at 37.5 °C, the IFN γ immunosensor was carefully washed with PBS. The R_{ct} value reflects the state of the electrode surface. After the formation of an aptamer monolayer with pentanethiol on the electrode, R_{ct} greatly increased compared to that of the bare electrode since the negative charge on the phosphate backbone and the steric hindrance of IFN γ interfered with the movement of the $[\text{Fe}(\text{CN})_6]^{3-/4-}$ ions [26]. The relative variation in the impedance of the immunosensor was investigated in PBS solution (0.1 M, pH 7.0) that contained KCl (0.1 M) and 5 mM $\text{K}_3[\text{Fe}(\text{CN})_6]/\text{K}_4[\text{Fe}(\text{CN})_6]$.

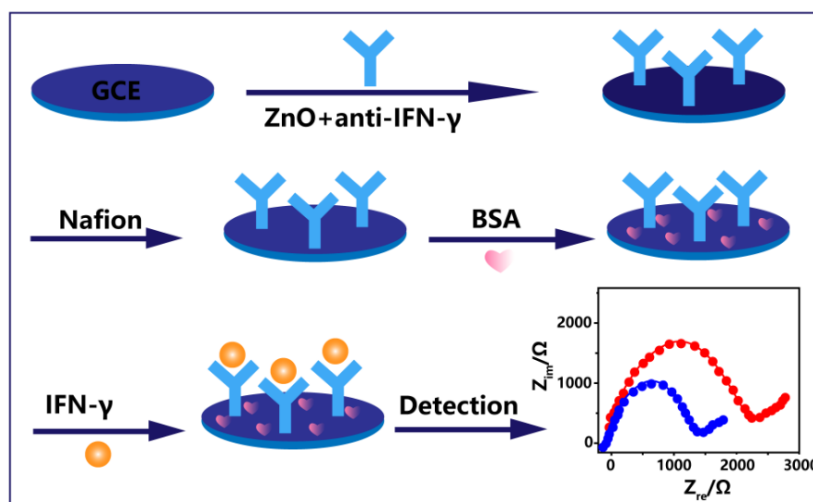


Figure 2. Schematic illustration of the immunosensor preparation process and the immunoassay of IFN γ .

The impedance variations between the modification steps were determined using EIS measurements. In the Nyquist plot of an impedance spectrum, the semicircle diameter can be used for the quantification of the electron transfer resistance (R_{ct}). Faradaic impedance spectra were recorded after the stepwise modification processes and are shown in Fig. 3A. Unlike under neutral conditions, in a high-pH buffer, the negative surface charge and the steric hindrance of IFN- γ increased with increasing IFN- γ concentration. These effects made the redox reaction of $[\text{Fe}(\text{CN})_6]^{3-/4-}$ more difficult;

therefore, the R_{ct} value increased [27]. The original GCE exhibited an insignificant semicircle, suggesting that the transfer resistance was low. An insignificant increase in R_{ct} was observed after modification of the GCE with TiO_2 NPs, suggesting that the TiO_2 NPs were attached to the surface of the electrode. An obvious increase in R_{ct} was observed upon loading the IFN- γ antibody onto the TiO_2 NP/GCE surface, implying that the antibody was successfully loaded onto the TiO_2 NPs. An additional increase in R_{ct} was observed after the blockage of the IFN- γ antibody-immobilized electrode using BSA. During the determination of the IFN γ antigen concentration using the immunosensor, a similar increase was also recorded, possibly due to the significant hindrance of the diffusion of the ferricyanide probe to the electrode surface by the protein layer formed on the electrode surface.

An FRA software (Autolab)-based Randles equivalent circuit was used for fitting the impedance data. As showed in Fig. 3B, the measured spectra were fit to the equivalent circuit and a modified Randles equivalent circuit, suggesting the desirable consistency between the measurement system and the circuit model throughout the tested frequency range. The circuit was comprised of the Warburg impedance (Z_w), electron transfer resistance (R_{ct}), solution resistance (R_s), and interfacial double layer capacitance (C_{dl}) between a solution and an electrode. Ordinarily, Z_w represents the diffusion properties of the redox probe in solution, while R_s corresponds to the bulk features of the electrolyte solution. Both parameters were unaffected by surface modification. These increases of R_{ct} values correspond to the loading of IFN- γ on the aptamer probe located on the electrode. Thus, these results clearly show that IFN- γ could be sensitively detected using this aptamer-based electrochemical impedance spectroscopy strategy [28]. The impedance data were fit the a Randles equivalent circuit using the constant phase element (CPE) rather than the classical capacitance because the C_{dl} electrode/electrolyte interface in this work was not a simple capacitor.

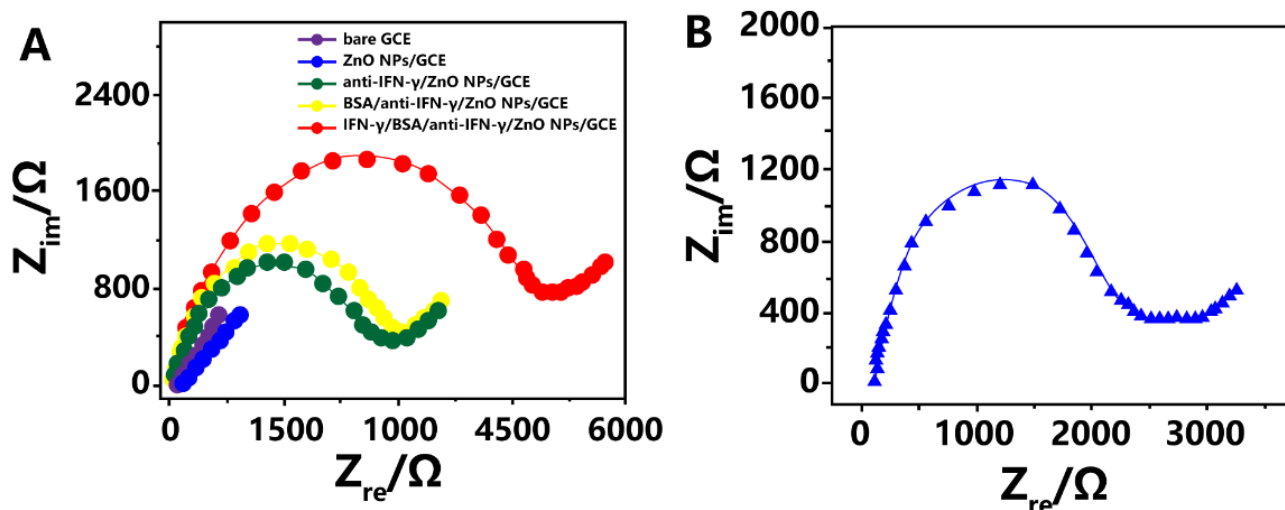


Figure 3. (A) Nyquist plots of the original GCE, the TiO_2 NP-modified GCE, the anti-IFN γ / TiO_2 NP-modified GCE, the BSA/anti-IFN γ / TiO_2 NP-modified GCE and the IFN γ /BSA/anti-IFN γ / TiO_2 NP-modified GCE in 0.1 M pH 7.0 PBS solution that contained KCl (0.1 M) and $\text{K}_3[\text{Fe}(\text{CN})_6]/\text{K}_4[\text{Fe}(\text{CN})_6]$ (5.0 mM). Scan rate: 50 mV/s. (B) Fitted and experimental Nyquist plots of the impedance spectra.

The interface characteristics of the electrode would not vary upon the capture of the target protein on the TiO₂ NPs/GCE, further causing a variation in R_{ct} . Hence, optimization of the parameters that affected the antibody-antigen reaction was carried out, which included the incubation time, incubation temperature, and solution pH. The effect of the solution pH on the relative variation in R_{ct} during the antigen-antibody reaction in the presence of IFN γ (0.01 ng/mL) is presented in Fig. 4A. An increase in ΔR_{ct} was observed as the solution pH increased in the range of 4.0 - 9.0 and then reached a plateau at a pH of 7.0. Therefore, pH 7.0 was selected as the optimized pH value for the immunoreaction. We also studied the effect of the incubation temperature in the range of 25 to 45 °C in the presence of IFN γ (0.01 ng/mL). Under two different pH conditions, a negative peak representing the helices of IFN- γ was commonly detected. These results confirm that the conformation of the IFN- γ antibody did not significantly change at high pH [29]. When the incubation temperature was 37.5 °C, the relative change in R_{ct} reached the maximum value (Fig. 4B). In addition, the Ag-Ab combination was significantly influenced by the incubation time; hence, we investigated the effect of the reaction time on the ΔR_{ct} value in the presence of IFN γ (0.01 ng/mL), as showed in Fig. 4C. An increase in the electrochemical response to the binding reaction was observed as the incubation time was prolonged, and then the response remained stable when the incubation time exceeded 80 min. Based on these results, the optimum incubation time, incubation temperature, and pH were determined to be 80 min, 37.5 °C, and 7.0, respectively, to achieve optimized IFN γ detection.

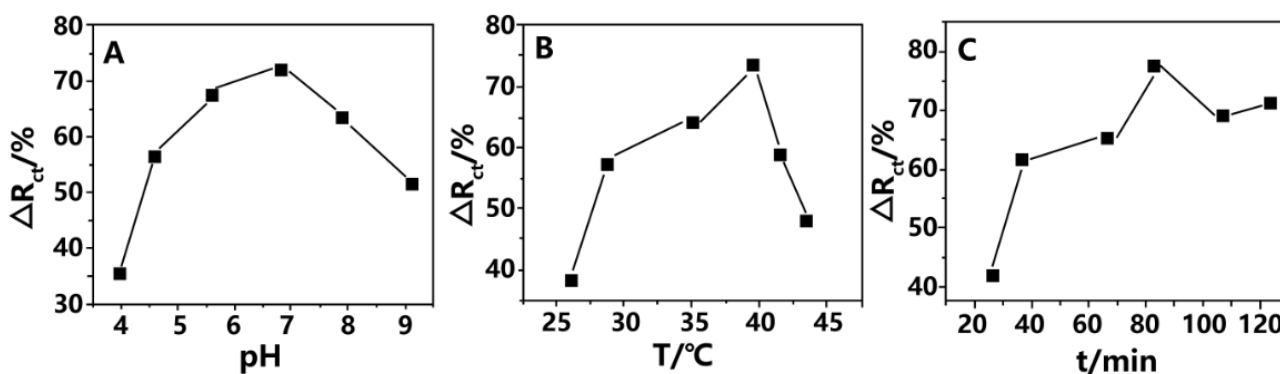


Figure 4. Effect of (A) solution pH, (B) incubation temperature and (C) incubation time on the relative variation in R_{ct} in the presence of IFN γ (0.01 ng/mL).

Our developed immunosensor was incubated with IFN γ at varying concentrations under the optimized conditions. The corresponding Nyquist plots of the impedance spectra are presented in Fig. 5A. As the IFN γ concentration increased, an increase in the semicircle diameter in the Nyquist plot was observed. The logarithm of IFN γ was found to be linearly related to the relative variation in R_{ct} , as showed in Fig. 5B. In addition, the LOD was estimated to be 0.74 pg/mL (S/N=3). The analytical features of our developed biosensor are compared with those of previous studies in Table 1.

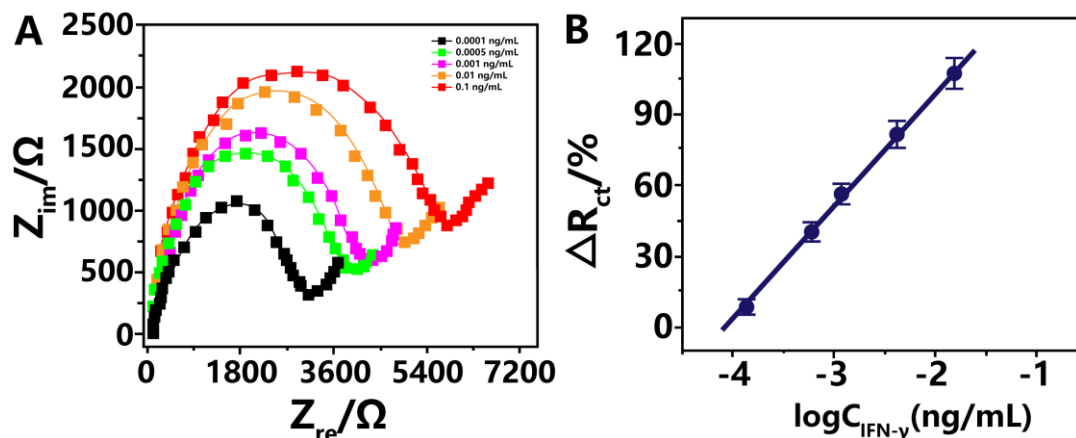


Figure 5. (A) Faradaic impedance spectra of our developed immunosensor after incubation with IFN γ (0.001, 0.005, 0.01, 0.1 and 0.2 ng/mL) in a PBS solution. (B) Calibration curve for IFN γ .

Table 1. Comparison of the major characteristics of electrochemical sensors used for the detection of AFP.

Electrode	Linear detection range	Detection limit	Reference
5'-thiol-modified aptamer probe /gold electrode	-	1 pM	[30]
Sandwich enzyme immunoassay	-	25 pg/mL	[31]
Aptamer-based array	1–500 ng/mL	1.3 ng/mL	[32]
IFN γ /BSA/anti-IFN γ /TiO $_2$ NPs	0.0001-0.1 ng/mL	0.74 pg/mL	This work

Intra- and inter-assay coefficients of variation (CVs) were used to assess the reproducibility of the developed immunosensor in IFN γ detection. The intra-assay CV obtained after six replicative measurements in the presence of IFN γ (0.01 ng/mL) was 3.4%, suggesting that the detection of the IFN γ immunosensor was highly reproducible. The inter-assay CV for six immunosensors prepared in six batches in the presence of IFN γ (0.01 ng/mL) was 3.2%, suggesting that the preparation of the IFN γ immunosensor was highly reproducible. This IFN γ immunosensor was stored in a refrigerator at 4 °C for further use. Our developed immunosensor showed no significant variation in the relative change in R_{ct} after being stored for 30 days. It is obvious that the as-prepared TiO $_2$ NPs provided a desirable microenvironment, thus helping the immobilized antibody molecules to maintain their bioactivity.

IFN γ (0.002, 0.005, 0.01, 0.05 and 0.1 ng/mL) was spiked into bovine serum specimens to assess the accuracy and feasibility of our proposed IFN γ immunosensor. Table 2 shows the recoveries, which suggested that our developed electrochemical impedance immunosensor could provide a highly accurate, label-free method for the determination of IFN γ in real specimens.

Table 2. Recoveries of IFN γ by the proposed electrochemical impedance immunosensor.

Sample	Added (ng/mL)	Found (ng/mL)	Recovery (%)	RSD (%)
1	0.005	0.0052	104	2.5
2	0.01	0.0108	108	3.1
3	0.05	0.0504	100.8	1.5
4	0.1	0.0983	98.3	0.7

4. CONCLUSIONS

This report presented a highly sensitive IFN γ detection method using a TiO $_2$ NP-based electrochemical impedance immunosensor prepared from a simple hydrothermal strategy. The IFN γ monoclonal antibody was immobilized on the TiO $_2$ NP/GCE, contributing to the successful preparation of an effective immunosensor. Our developed immunosensor was easy to use, highly sensitive, stable, reproducible, and specific. In addition, this immunosensor possessed a broad linear range, was highly accurate and could be used for the determination of IFN- γ in real specimens, as shown in the recovery test.

References

1. A. Antonelli, M. Rotondi, S. Ferrari, P. Fallahi, P. Romagnani, S. Franceschini, M. Serio and E. Ferrannini, *The Journal of Clinical Endocrinology & Metabolism*, 91 (2006) 614.
2. M. de Carli, M. D'Elis, S. Mariotti, C. Marcocci, A. Pinchera, M. Ricci, S. Romagnani and G. del Prete, *The Journal of Clinical Endocrinology & Metabolism*, 77 (1993) 1120.
3. J. Aniszewski, R. Valyasevi and R. Bahn, *The Journal of Clinical Endocrinology & Metabolism*, 85 (2000) 776.
4. P. Romagnani, M. Rotondi, E. Lazzeri, L. Lasagni, M. Francalanci, A. Buonamano, S. Milani, P. Vitti, L. Chiovato and M. Tonacchera, *The American Journal of Pathology*, 161 (2002) 195.
5. A. Antonelli, M. Rotondi, P. Fallahi, P. Romagnani, S. Ferrari, A. Buonamano, E. Ferrannini and M. Serio, *The Journal of Clinical Endocrinology & Metabolism*, 89 (2004) 5496.
6. A. Antonelli, M. Rotondi, P. Fallahi, P. Romagnani, S.M. Ferrari, A. Paolicchi, E. Ferrannini and M. Serio, *European Journal of Endocrinology*, 152 (2005) 171.
7. M. García-López, D. Sancho, F. Sánchez-Madrid and M. Marazuela, *The Journal of Clinical Endocrinology & Metabolism*, 86 (2001) 5008.
8. M. Rotondi, E. Lazzeri, P. Romagnani and M. Serio, *Journal of Endocrinological Investigation*, 26 (2003) 177.
9. Y. Lin, J. Luo, C. Chiou, C. Yang, C. Wang, C. Chou and C. Lai, *Sensors and Actuators B: Chemical*, 186 (2013) 374.
10. P. Kumar, S. Maikap, A. Prakash and T. Tien, *Nanoscale Res Lett*, 9 (2014) 179.
11. Y. Lin and P. Peng, *Anal. Chim. Acta.*, 869 (2015) 34.
12. Y. Lin, S. Wang, M. Wu, T. Pan, C. Lai, J. Luo and C. Chiou, *Biosensors and Bioelectronics*, 43 (2013) 328.
13. T. Pan, C. Wang, Y. Huang, W. Weng and S. Pang, *Journal of The Electrochemical Society*, 162 (2015) B83.
14. J. Her, M. Wu, Y. Peng, T. Pan, W. Weng, S. Pang and L. Chi, *Int. J. Electrochem. Sci*, 8 (2013)

606.

15. S. Schusser, A. Poghossian, M. Bäcker, M. Krischer, M. Leinhos, P. Wagner and M.J. Schöning, *Sensors and Actuators B: Chemical*, 207 (2015) 954.
16. M. Huang, H. Li, H. He, X. Zhang and S. Wang, *Analytical Methods*, 8 (2016) 7413.
17. K. Miyamoto, K. Hayashi, A. Sakamoto, C. Werner, T. Wagner, M. Schöning and T. Yoshinobu, *Sensors and Actuators B: Chemical*, 248 (2017) 1006.
18. R. Packard, X. Zhang, Y. Luo, T. Ma, N. Jen, J. Ma, L. Demer, Q. Zhou, J.W. Sayre and R. Li, *Annals of Biomedical Engineering*, 44 (2016) 2695.
19. W. Weng, C. Wang, S. Pang and T. Pan, *Journal of The Electrochemical Society*, 163 (2016) B445.
20. S. Beging, M. Leinhos, M. Jablonski, A. Poghossian and M.J. Schöning, *Physica Status Solidi (a)*, 212 (2015) 1353.
21. A. Poghossian, M. Weil, A.G. Cherstvy and M.J. Schöning, *Anal Bioanal Chem*, 405 (2013) 6425.
22. T. Pan and C. Tan, *Journal of Materials Chemistry C*, 4 (2016) 7436.
23. S. Patskovsky, V. Latendresse, A. Dallaire, L. Doré-Mathieu and M. Meunier, *The Analyst*, 139 (2013) 596.
24. G. Lui, J. Liao, A. Duan, Z. Zhang, M. Fowler and A. Yu, *Journal of Materials Chemistry A*, 1 (2013) 12255.
25. M. Dijkema, B. Kamp, J. Hoogvliet and W. Van Bennekom, *Analytical Chemistry*, 73 (2001) 901.
26. A. Schmittel, U. Keilholz and C. Scheibenbogen, *Journal of Immunological Methods*, 210 (1997) 167.
27. M. Reynard, D. Turner and C. Navarrete, *International Journal of Immunogenetics*, 27 (2000) 241.
28. M. Santin, L. Munoz and D. Rigau, *PloS one*, 7 (2012) e32482.
29. Y. Zhang, B. Zhang, X. Ye, Y. Yan, L. Huang, Z. Jiang, S. Tan and X. Cai, *Materials Science and Engineering: C*, 59 (2016) 577.
30. K. Min, M. Cho, S. Han, Y. Shim, J. Ku and C. Ban, *Biosensors and Bioelectronics*, 23 (2008) 1819.
31. J. Rothel, S. Jones, L. Corner, J. Cox and P. Wood, *Australian Veterinary Journal*, 67 (1990) 134.
32. Y. Chen, T. Pui, P. Kongsuphol, K. Tang and S. Arya, *Biosensors and Bioelectronics*, 53 (2014) 257.